Vol. 15: 1–18, 2023
https://doi.org/10.3354/aei00448

AQUACULTURE ENVIRONMENT INTERACTIONS
Aquacult Environ Interact

Published January 19

Mussel farming production capacity and food web interactions in a mesotrophic environment

Paul Gatti, Antonio Agüera, Shuang Gao, Øivind Strand, Tore Strohmeier, Morten D. Skogen*

Institute of Marine Research, Pb-1870 Nordnes, 5817 Bergen, Norway

ABSTRACT: Low trophic aquaculture (LTA), such as bivalve farming, offers promising avenues to supply sustainable seafood and aquafeed. While bivalve farming usually occurs in highly productive coastal areas which already support numerous human activities and suffer from environmental pressures, numerical tools offer a promising avenue to explore and assess biomass production potential and associated ecosystemic impacts for further development of the industry and prospection of new exploitation sites. In this study, we coupled an ecophysiological model, the dynamic energy budget theory (DEB), with an ecosystem model (NORWECOM.E2E) to simulate blue mussel *Mytilus* spp. farming production and effects based on the food web in the mesotrophic Hardangerfjord in western Norway. We tested several levels of fjord-scale farming intensity and assessed 2 production purposes: aquafeed and human consumption. Results suggested the Hardangerfjord could host large-scale mussel farming for both purposes. However, large exploitation schemes displayed detrimental effects on individual mussel growth (39% less wet mass after 2 yr) and especially on secondary production (decrease of 33% after 1 yr) due to acute trophic competition. Simulations showed short production cycles for aquafeed were more efficient to exploit primary production, since young and small mussels have lower maintenance and reproduction costs. Dissolved nutrient inputs from salmonid farms had marginal effects on primary production (<2%). However, salmonid and mussel farming activities could compete for the sites with the highest production potential.

KEY WORDS: DEB model · IBM model · Blue mussel · Aquaculture · Mesotrophic · Food web · Hardangerfjord

1. INTRODUCTION

Supplying the growing demand for food by the human population while ensuring environmental sustainability of food production is one of the biggest challenges humanity is facing. In the movement towards sustainable food production, the expansion of low trophic aquaculture (LTA) is proposed as a potential route to obtain significantly more food and biomass from the ocean, both directly for human consumption and indirectly as ingredients in feed (SAPEA 2017). Farming herbivorous filter feeders, such as sessile bivalves, efficiently converts low trophic resources to nutritious food, as these graze on phytoplankton, other microorganisms, and organic detritus (Willer et al. 2021). Bivalves are typically farmed in coastal waters adjacent to populated areas and are globally one of the largest suppliers of food for human consumption out of mariculture (FAO 2020). Bivalve farming also provides socioeconomic services and development opportunities (Krause et al. 2019, Willer & Aldridge 2020). Recently, bivalves have been suggested as potential candidates to meet the increasing need for sustainable marine resources as ingredients in feed for e.g. salmonid production (Albrektsen et al. 2022). Such resources must have

*Corresponding author: morten@imr.no

Publisher: Inter-Research · www.int-res.com

high nutritional value as well as the capacity to efficiently exploit the large production potential of low trophic levels, which makes filter feeders like mussels ideal (Filgueira et al. 2019).

While bivalve production in Asia is growing, it is stabilizing or decreasing on other continents (Wijsman et al. 2019). Mussel production in the European Union has decreased over the last 2 decades; causes of the decline are presumed to be environmental factors, including available space, rather than economic factors (Avdelas et al. 2021). Conflicting activities and environmental pressure on coastal waters demand the consideration of other areas and ecosystems for LTA production, and an increasing interest in expansion to offshore sites and less exposed or unexploited coastal regions like meso-oligotrophic fjord areas has arisen (Strohmeier et al. 2009, Torrissen et al. 2018, Jansen et al. 2019, Galparsoro et al. 2020, Mascorda Cabre et al. 2021, Thomas et al. 2022). Remote sites, lack of infrastructure and insufficient conditions for culture may restrict such areas from being exploited. Compared to farming in coastal shallow waters, unexploited regions may represent ecosystems with greater depths, complex hydrodynamics, and specific requirements to maximize production based on appropriate ecophysiological knowledge. Culture in unexploited meso-oligotrophic environments has been typically disregarded due to low food (seston) concentrations; nevertheless, recent ecophysiological research has shown the feasibility of culturing bivalves in such low seston environments (Rosland et al. 2009, 2011, Strohmeier et al. 2009, ICES 2022), suggesting vast unexploited areas may be useful for bivalve culturing. This knowledge has strengthened the argument for making bivalve farming in fjords a prime candidate for diversifying Norwegian aquaculture towards more low trophic species (Torrissen et al. 2018, ICES 2022).

Commercial-scale farming of mussels interacts with the environment and may affect the ecosystem by altering the nutrient compartments, trophic structure, and energy flow (Jansen et al. 2019). The Norwegian coast is characterized by having a variety of fjord systems. The intertidal and subtidal zones commonly inhabited by mussels in fjords are typically steeply sloped, rocky, hard substrates, making the area available for bivalve culture relative to the water volume of the fjord small compared to ecosystems in shallower coastal waters, where most farmed mussel production is located (Jansen et al. 2019). Introduction of farms with suspended longline for mussel production in fjords may therefore result in very high farmed biomass compared to the natural populations, which should be of concern for ecosystem impact assessments, research to inform policy, and development of management strategies for sustainable farming. As the pressure to increase low trophic production in unexploited areas increases, it is timely to assess the potential for large-scale farming considering both the production capacity and ecosystem effects on a regional level (Strand & Vølstad 1997).

Over the last 2 decades, numerical modelling tools coupling ecophysiology based on the dynamic energy budget (DEB) theory and environmental forcings based on field monitoring or physical–biogeochemical models have been widely implemented to explore the growth of bivalves or the productivity and carrying capacity of bivalve farming under varying local environments (Maar et al. 2015, 2020, Lavaud et al. 2020, Palmer et al. 2020, Pete et al. 2020, Saraiva et al. 2020, Taylor et al. 2021). DEB models simulate numerous ecophysiological functions of individuals, such as growth, spawning, food uptake, respiration, or egestion, as a function of environmental forcings, and may be extrapolated to farmed or wild populations using box models (e.g. Filgueira et al. 2016, Pete et al. 2020) or individual based models (IBMs) (e.g. Filgueira et al. 2014, Saraiva et al. 2014, Thomas et al. 2020). These models enable the simulation of feedback from shellfish populations through the direct effect on phytoplankton biomass of grazing and the indirect effect of nutrient recycling via egestion. Thus, the full bidirectional integration of DEB-IBMs with high resolution biophysical models produces tools that can be used to describe the impact of the environment on populations of the studied species, while at the same time incorporating the effects of these populations on the environment.

In the present study we have applied the high-resolution 3D ecosystem model NORWECOM.E2E (Skogen et al. 1995) extended and 2-way coupled with an individual based model (IBM) integrating a DEB module for the blue mussel *Mytilus* spp. complex (Kotwicki et al. 2021). The model system is used to build scenarios of fjord-scale intensive mussel farming in the Hardangerfjord. High resolution models have previously been extensively applied in carrying capacity assessments of salmonid farming and management development in this fjord system in relation to salmon lice (e.g. Sandvik et al. 2020), and, coupled with the NORWECOM.E2E ecosystem model, with respect to eutrophication (Skogen et al. 2009). We simulated large-scale mussel farming to assess growth and production potential from farming cycles

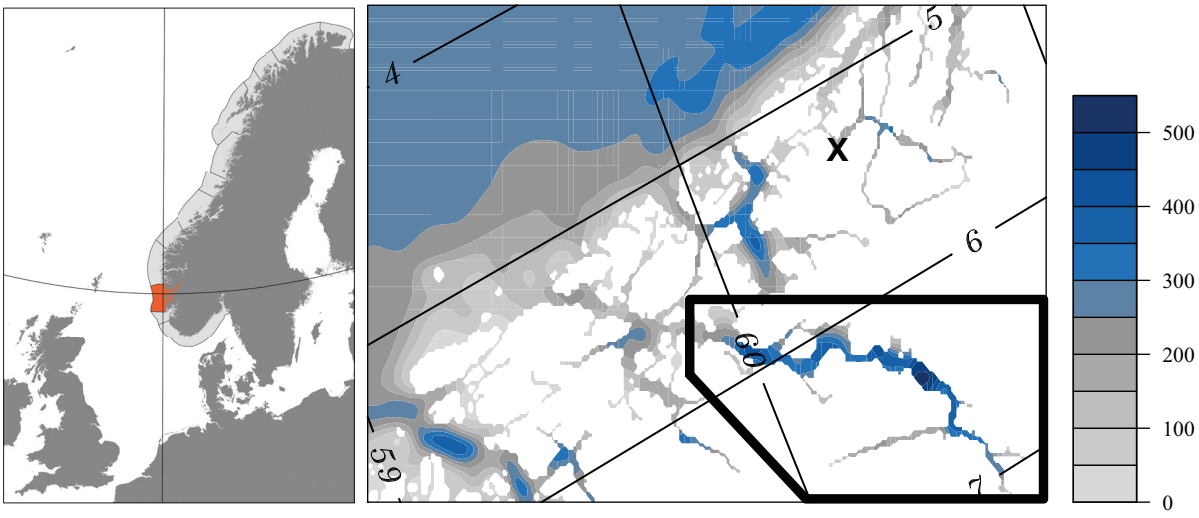

Fig. 1. Hardanger area and model domain with bathymetry (m). The black box is the area assessed for possible mussel farms (also used for the statistics of primary and secondary production), and X indicates the location of Bergen

for feed ingredients and human consumption. Further, the effects on the mesotrophic food web, with respect to impacts on planktonic primary and secondary producers, were studied. A scenario removing the dissolved nutrient contribution from salmon farms was added to assess possible interactions and options for area co-use at regional scales.

2. MATERIALS AND METHODS

2.1. Study area

The Hardangerfjord, in southwest Norway (Fig. 1), stretches 180 km inland from the coast. Sill depth is ca. 170 m, and the fjord has several deep basins, with a maximum depth of 850 m. With several connections to the open sea and many fjord arms receiving freshwater input from land, the current pattern is relatively complicated, with large temporal and spatial variability. A description of the fjord physics in detail (temperature, salinity, and currents) can be found in Asplin et al. (2014) and Johnsen et al. (2014).

2.2. Physical model

The hydrodynamic model for the Norwegian coast (NorKyst800) (Albretsen et al. 2011) is an automation of the numerical ocean model ROMS (Regional Ocean Modeling System; http://myroms.org, Shchepetkin & McWilliams (2003, 2005)), implemented with a horizontal resolution of 800 m and suitable sources of forcing (including high resolution atmospheric forcing, tides, and rivers) as described by Asplin et al. (2014). NorKyst800 has been proven to generate realistic results for currents, salinity, and temperature (Asplin et al. 2020).

2.3. NORWECOM.E2E model

The NORWegian ECOlogical Model system End-To-End (NORWECOM.E2E) is a merger of a nutrient-phytoplankton-zooplankton-detritus (NPZD) model for nutrient and plankton cycling (Aksnes et al. 1995, Skogen et al. 1995) and different IBMs developed initially for fish (Utne et al. 2012) and zooplankton (Hjøllo et al. 2012). NORWECOM.E2E combines all these components into one integrated model where one can use all or a selected number of modules in a simulation.

In the present study, the NPZD model used is 2-way, coupled to a newly developed IBM for mussels where the core computational part is a mussel DEB model (Section 2.4). The model runs in offline mode, taking physical ocean fields (velocities, salinity, temperature, water level, and sea-ice) from the NorKyst800 model (Fig. 2). In the vertical dimension 21 sigma-layers are used, and the time step is 300 s.

The NPZD model is coupled to the physical model through light, hydrography, and the movement of water masses. The prognostic variables are dissolved inorganic nitrogen (nitrate, nitrite, ammonia), phosphorus (phosphate) and silicate, 2 types of phytoplankton (diatoms and flagellates), 2 detritus pools (particulate nitrogen and phosphorus), diatom skeleton (biogenic silica), oxygen, and 2 types of zoo-

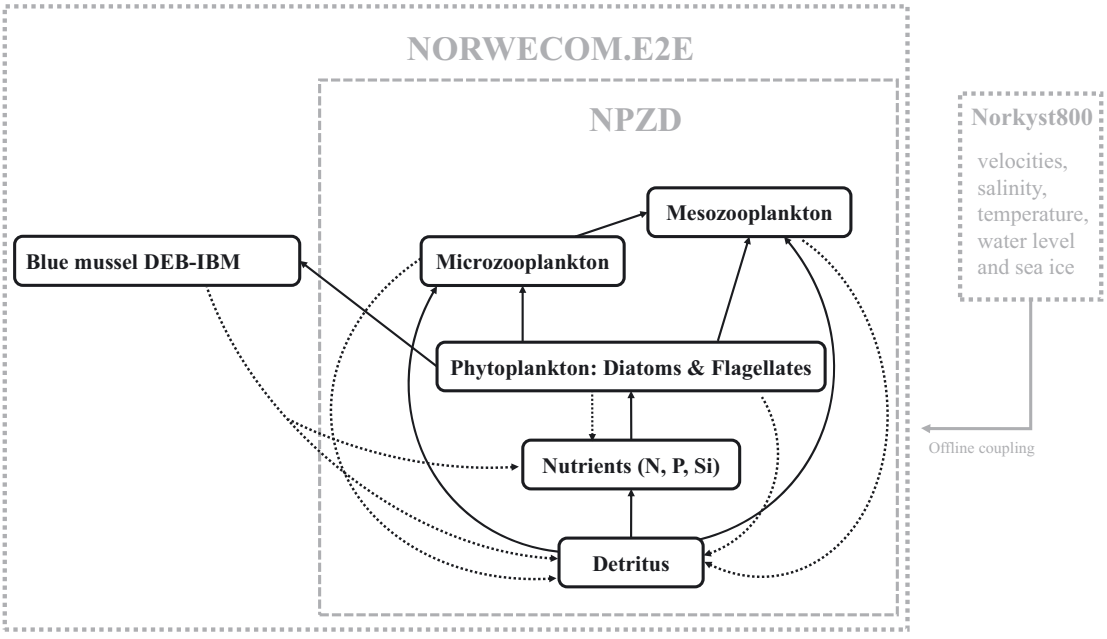

Fig. 2. Conceptual scheme of the NORWECOM.E2E model. Solid lines represent uptake via grazing, while dotted lines represent loss terms linked to grazing, such as egestion and excretion

plankton (meso- and microzooplankton). The latter variables are based on a module from the ECOHAM4 model (Moll & Stegert 2007, Pätsch et al. 2009, Stegert et al. 2009). The processes included are primary and secondary production, respiration, algal death, remineralization of dead organic matter, self-shading, turbidity, sedimentation, resuspension, sedimental burial, and denitrification. Remineralization takes place both in the sediments and in the water column. Particulate matter may accumulate on the bottom or become resuspended dependent on the bottom stress. Parameterization of biochemical processes is taken from the literature (Garber 1984, Pohlmann & Puls 1994, Aksnes et al. 1995, Gehlen et al. 1995, Lohse et al. 1995, 1996, Mayer 1995, Bode et al. 2004). All calculations are done in nitrogen units (mgN m^{-3}) using the Redfield ratio to calculate phosphorus and silicate fluxes.

The incident irradiation is formulated based on Skartveit & Olseth (1986, 1987) using shortwave radiation outputs from the ROMS simulation. Typical winter nutrient concentrations for the Hardangerfjord (inorganic nitrogen, phosphorus, and silicate = 6.0, 0.35, and 2.7 µmol l^{-1}, respectively) are taken from the Institute of Marine Research database and used as initial fields for the whole fjord together with a small amount of phyto- and zooplankton (0.1 mgN m^{-3}). Winter nutrient concentrations for the North Sea are taken from an existing NORWECOM.E2E simulation (Gao et al. 2021), and these values are also used at the open boundaries. Hordaland county (including Hardangerfjord) is a core area for salmonid fish farming in Norway, with an annual production close to 200 kt. Loads of dissolved inorganic nutrients (N and P) from all farms are included based on production estimates for 2019 from the Norwegian Directorate of Fisheries (www.fiskeridir.no), while no river inputs of nutrients are included. To get an initial nutrient field in dynamic balance with the physics, the model was first spun-up for 2 full years starting on January 1, 2018, repeating the 2018 forcing. The nutrient and plankton fields on the last day were then stored and used as the initial field in the remaining simulations. To absorb inconsistencies between the forced boundary conditions and the model results, a 7 grid-cell flow relaxation scheme (FRS) zone (Martinsen & Engedahl 1987) was used around the open boundaries.

2.4. Mussel DEB-IBM

The dynamics of mussel biomass are predicted as multiple individuals representing a farm situation, where one farm is modelled as a single super individual (SI, Scheffer et al. 1995), i.e. an aggregation of numerous individuals sharing the same characteristics (e.g. same birth date or size). The life cycle of mussels is modelled following DEB theory (Kooijman 2010). The DEB model is a mechanistic bio-energetic

model that describes energy fluxes occurring within an organism to predict its development, growth, reproduction, and ultimately death as a response to environmental forcing (e.g. temperature and food availability). The DEB model implemented in this study accounts for metabolic acceleration occurring between birth and metamorphosis, also known as the 'abj' model (Marques et al. 2018).

The mussel DEB-IBM model is coupled to the NPZD model through the ingestion of phytoplankton, subsequent egestion of nutrients, and detritus production. Ingestion is estimated from the concentration of phytoplankton at the vertical positioning of the farms. There is no direct competition between mussels within a farm; thus each individual in a SI has the same amount of food. The competition process is mainly restricted to food depletion and competition between farms. The NPZD model reports phytoplankton biomass in nitrogen units, and these are converted to carbon used in the mussel model using a C:N molecular ratio of 122:16 (Rey et al. 2000). The grazed phytoplankton is mainly regenerated through the detritus pool, but to mimic excretion and egestion, 10% is instantly regenerated as dissolved inorganic nitrogen (in nature as ammonium) and 25% as phosphorus available for further uptake by the phytoplankton (Garber 1984, Bode et al. 2004).

Ingestion in the mussel DEB model deviates from the standard DEB model by using a Holling's type III functional response instead of the standard Holling's type II accounting for the characteristics of the environment and mussel feeding physiology (Strohmeier et al. 2009). Captured food particles are then ingested and digested. Assimilated energy is stored in the energy reserves (E) (Fig. 3). Reserves are then mobilized and allocated to both structural volume (V, somatic growth and maintenance) and maturity level (H, while the individual is immature) or reproductive reserves (R, for a mature individual), as well as associated maintenance costs, following a fixed fraction known as the K-rule. Maintenance costs are taken first and what is left is allocated to V and H or R. Starvation may occur when food availability is low, i.e. when the energy mobilized from the reserve (E) is not sufficient to fuel maintenance. Departures from the DEB standard are necessary to avoid death in such conditions; for instance the energy required to pay maintenance cost may be taken from either V (shrinking) or R (Bernard et al. 2011, Gatti et al. 2017, Buer et al. 2020, Thomas et al. 2020). In the case of adult mussels, it is known they prioritize maintenance of the reproductive buffer over somatic tissue

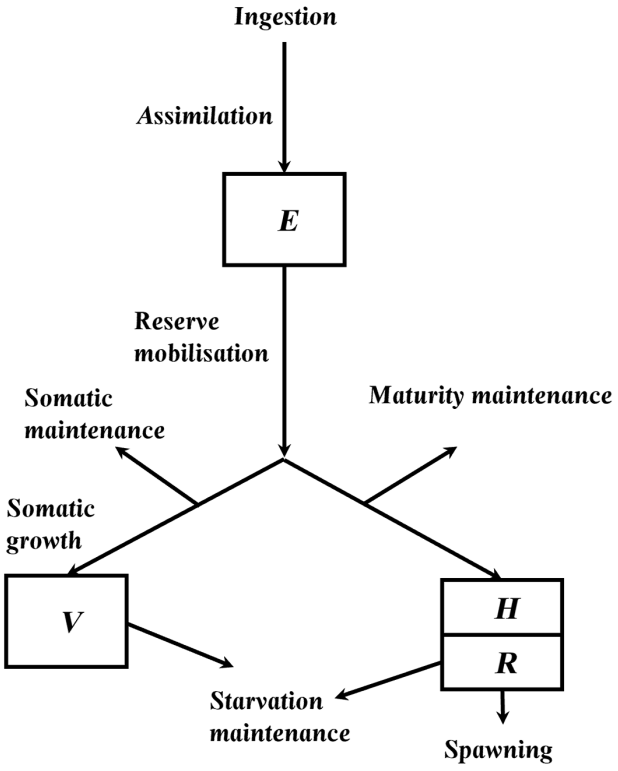

Fig. 3. Dynamic energy budget diagram illustrating energetic fluxes. E: energy reserves; V: structural volume; H: maturity level; R: reproductive reserves

during short-term starvation (Pipe 1985). As such, when mussels enter starvation in this DEB model, energy is at first re-mobilized from V until $V = 0.7 \times V'$ (with $V' = \max(V, V')$ a shrinking free volume). Beyond that threshold, R are used until exhaustion and ultimately death. In case of juveniles, as they have not built R yet, V is re-mobilized until $V = 0.7 \times V'$; beyond that the individual dies. The $0.7 \times V'$ threshold is based on empirical observations of weight loss over 2 mo (Pipe 1985) in overwintering populations in Hardangerfjord, and the model assumes a 100% efficiency of energy remobilization (from either V or R). Mortality sources, other than starvation, are assumed to be negligible.

In western Norway, Duinker et al. (2008) reported that *Mytilus edulis* display 2 spawning events in spring and autumn, characterized by scattered spawning between April and May, a peak in late June–early July, and a second spawning event in September. Thus, in the model, mussel spawning is enabled between April and September. Spawning is only triggered for individuals older than 6 mo with a gonado-somatic index (GSI) above 0.3 (Maar et al. 2009). Once spawning is triggered, reproductive reserves are used to release gametes. To reduce the

risk of starvation events, after spawning in early spring, we introduced an additional rule stating that only 90 % of R is used for each spawning event and the remaining 10 % is kept as a buffer. Here, we only focus on the energetic loss of gametes, and they are not fertilized.

Equations and parameter values are provided in Sections S1–S10 in the Supplement at www.int-res.com/articles/suppl/q015p001_supp.pdf. The model was calibrated using the covariation method (Lika et al. 2011a,b, Marques et al. 2019) using the same sets of data used by Rosland et al. (2009), i.e. data on growth of mussel shell and mass, clearance rates, and ingestion rates, along with environmental temperature and seston particulate organic carbon. Data for larvae growth and clearance rate at different temperatures and food levels was sourced from the work of Sprung (1984a,b,c,d). Other data observations (GSI, maximum size, etc. are given with references in Table S1, and a comparison between observed and modelled dry mass and shell length is given in Fig. S1. Model fitness is mean relative error (MRE) = 0.336 and sum of symmetric mean squared error (SMSE) = 0.314.

2.5. Experimental set-up

Potential sites for mussel farming were identified as grid cells fulfilling the following criteria: (1) average surface current speed above 6 cm s^{-1} to support seston (food) supply conditions, and (2) next to land or 2 grid points from land with the additional requirement of bottom depth less than 50 m, a conservative estimate of the maximum depth at which a farm can be anchored.

All sites within the box in Fig. 1 matching these criteria are shown in Fig. 4A. An initial simulation was done to allow for a selection of the best 100 sites. These were initialized on June 1, 2018, with one SI containing 1 million juveniles in each site. As mussels are normally farmed within a depth range of 1 to 7 m, a fixed farm depth of 4 m was used. DEB state variable values of an individual that just completed settlement were used for initialization values (see Table 1), and farms were assessed according to their

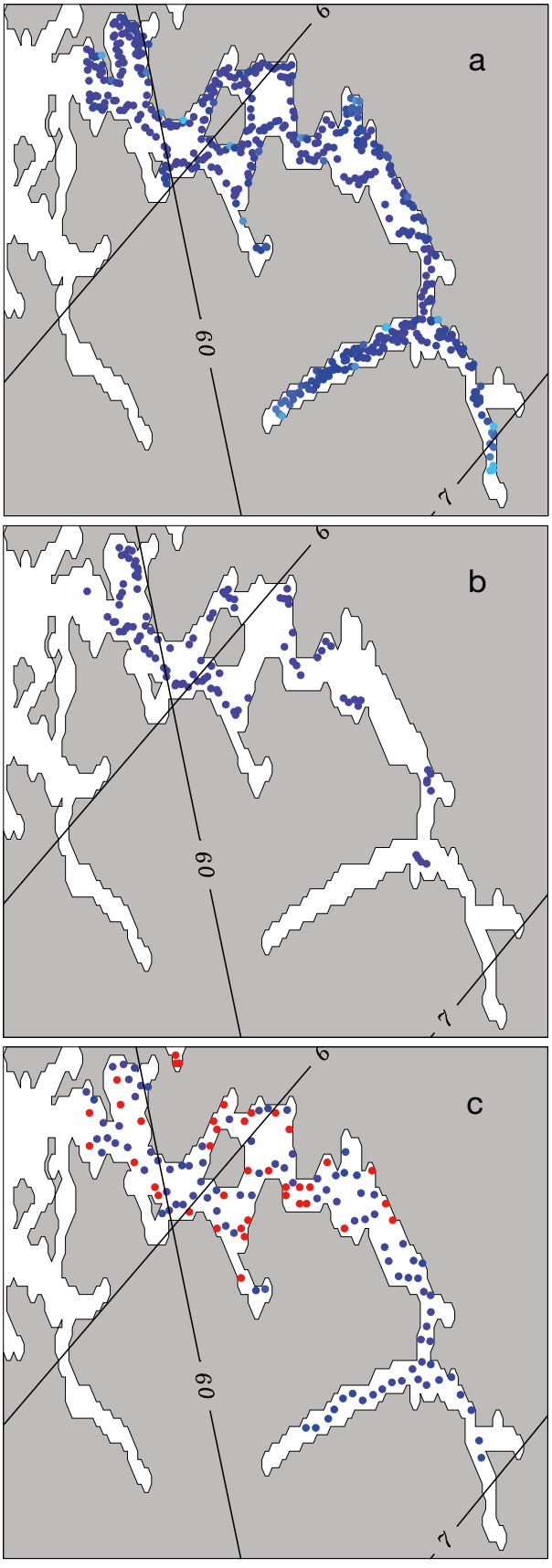

Fig. 4. Site selection. (a) All possible sites for mussel farms, (b) the 100 best sites in terms of production potential, and (c) the 100 best sites meeting the constraint of a minimum 1.6 km distance between farms. Colors indicate structural volume (V, as a proxy of growth) with darkest blue the highest. Red dots show existing sites of fish farms

Table 1. DEB state variables and parameters describing a recently settled individual, used as initial status for the model

Variable	Symbol	Value	Unit
Energy reserves	E	9.551025×10^{-4}	J
Structural volume	V	4.647640×10^{-7}	cm^3
Maturity level	H	$E_{Hj} = 0.0121$	J
Reproductive reserves	R	0.0	J
Acceleration factor	s_M	3.255917	–

structural volume (V) on December 31, 2019. We chose V as a proxy of growth (in length or weight). V is less sensitive than the overall energy content or flesh mass to the feeding condition and spawning phenology and thus displays a more monotonic trend.

Since some of the 100 selected sites were only 1 or 2 grid cells apart, we introduced a regulatory criterion based on minimum required distance between the farms, implemented to reduce risk of connectivity and disease transfer. In general, this accounts for the distance between both fish farms already operating in the area and mussel farms. In the present study, a minimum distance of 1.6 km (2 grid cells) was used (Norwegian Ministry of Trade, Industry and Fisheries 2015). Finding the 100 best sites with this extra criterion is in graph theory called the maximum independent set problem and is known to be NP-hard (https://www.baeldung.com/cs/p-np-np-complete-np-hard). Therefore, to solve it, a simple heuristic was used. First, the best site in the set of all valid sites was selected and its neighbors within 1.6 km were removed from the set. The algorithm was then repeated for the remaining set until 100 sites were chosen.

Production and interactions with the food web were then explored using a set of simulations with various stock densities (S0–S6; Table 2). For all simulations, juveniles were initiated after metamorphosis on the 100 selected best sites (Fig. 4C) as defined in Table 1 on June 1, 2018, using a 1 yr production cycle for feed (until September 1, 2019) and a 2 yr production cycle for human consumption (until September 1, 2020).

Source code is available at git.imr.no/norwecome2e in Fortran (F90) version f0c1e72. Post-processing of simulations was performed in R (R Core Team 2019).

2.6. Indicators and metrics

The growth potential of the mussels was assessed using 2 different metrics: total wet weight and shell length. Total wet weight (W_{tw}), which also includes shell weight, is given as

$$W_{tw} = \left(V \cdot d_V + E \cdot \frac{\omega_E}{\mu_E} + R \cdot \frac{\omega_R}{\mu_R}\right) \cdot \frac{1}{WD} \quad (1)$$

where d_V is the structure specific density, ω and μ are the molecular weights and chemical potential for the energy reserves and reproduction reserves, respectively (see Table S1) and $WD = 0.048$ (g g^{-1}) is a conversion factor from total wet mass to shell free dry mass. The overall production in each scenario is then simply the sum of all mussel weights within all farming sites. Shell length (sl) is given as

$$sl = \frac{\sqrt[3]{V'}}{\delta_M} \quad (2)$$

where δ_M is a shape coefficient (0.2582, Table S1). In the analysis, growth in shell length was assessed towards target commercial sizes of 4.0 to 5.0 cm (H. Sveier pers. comm.) for feed production and 6.0 cm for human consumption.

Further, the proportion of carbon fixed into mussel flesh relative to the amount of ingested phytoplankton carbon (r_C, mol mol^{-1}) was estimated to assess the efficiency of biomass conversion from phytoplankton to mussel

$$\begin{cases} r_C = \dfrac{MusselC - MusselC_{init}}{IngestedC} \\ MusselC = V \cdot d_V / \omega_E + (E + R)/\mu_E \\ IngestedC = \dfrac{\Sigma_t p_A}{\mu_X \cdot \kappa_x} \end{cases} \quad (3)$$

where μ_X is the food chemical potential and κ_X is the digestion efficiency of food to reserves (Table S1).

Note that since the organic compounds (X [= food], E, V, R) have a fixed C:N ratio (Kooijman 2010), budgets in nitrogen and carbon are proportional.

Finally, to assess the potential impact of farms on the food web, we looked at the

Table 2. Summary of scenarios of mussel farming intensity

Scenarios	Description
S0	Reference simulation. Only 1 juvenile in each mussel farm
S1	Very low biomass. 10 million juveniles per farm
S2	Low biomass. 25 million juveniles per farm
S3	Medium biomass. 50 million juveniles per farm
S4	High biomass. 100 million juveniles per farm
S5	Very high biomass. 200 million juveniles per farm
S6	Like S5 but without extra nutrients from fish farms

total phytoplankton uptake (carbon mass) by mussels and the effect on net primary and secondary production in the NPZD model.

3. RESULTS

3.1. Site selection

Potential sites for mussel farms are distributed along the entire fjord except for some areas at the end of the fjord branches (Fig. 4A). The 100 best sites were mostly located in the outer area (Fig. 4B). Considering a minimum distance of 1.6 km between farms (including both mussel and salmon farms), the sites were redistributed more evenly over the fjord (Fig. 4C). This constraint led to a decrease of 8% of the overall *V* production potential compared to the optimal set of locations for mussels.

3.2. Mussel growth and production

Mussels reached an average total wet mass ranging from 6.4 (S6) to 8.2 g (S0) in September 2019 (after a 1 yr production cycle designed for feed production) and 12.1 to 19.8 g in September 2020 (after a 2 yr production cycle designed for human consumption) (Fig. 5). Corresponding shell lengths ranged from 4.6 to 4.9 cm for feed production and from 5.9 to 6.6 cm for human consumption. Average mussel growth in both total wet mass and shell length decreased with the intensity of farming, i.e. the initial concentration of mussel juveniles per farming site. All farming scenarios supported growth up to a target commercial size of 4.0 cm for feed production on most selected sites (Figs. 5 & 6). However, the target size of 5.0 cm by September 1, 2019 was not met for most sites or scenarios. As mussel growth mainly occurs within productive months (from spring to fall), growth up to a target size of 5.0 cm could delay harvesting farther into the fall or even as far as the following (2020) productive season in the case of S5 and S6 (Figs. 5 & 7). A smaller fraction of the sites in S5 supported the growth of mussels up to 5.0 cm by fall 2019 for feed production, in contrast to S0 (Fig. 5 & 7). A lot of these sites of lower production are in the inner fjord and are non-optimal when considering a minimum distance between farms (Fig. 4). With a target commercial size of 6.0 cm for human consumption, sufficient average growth by September 2020 was met in most scenarios excepting S5 and S6,

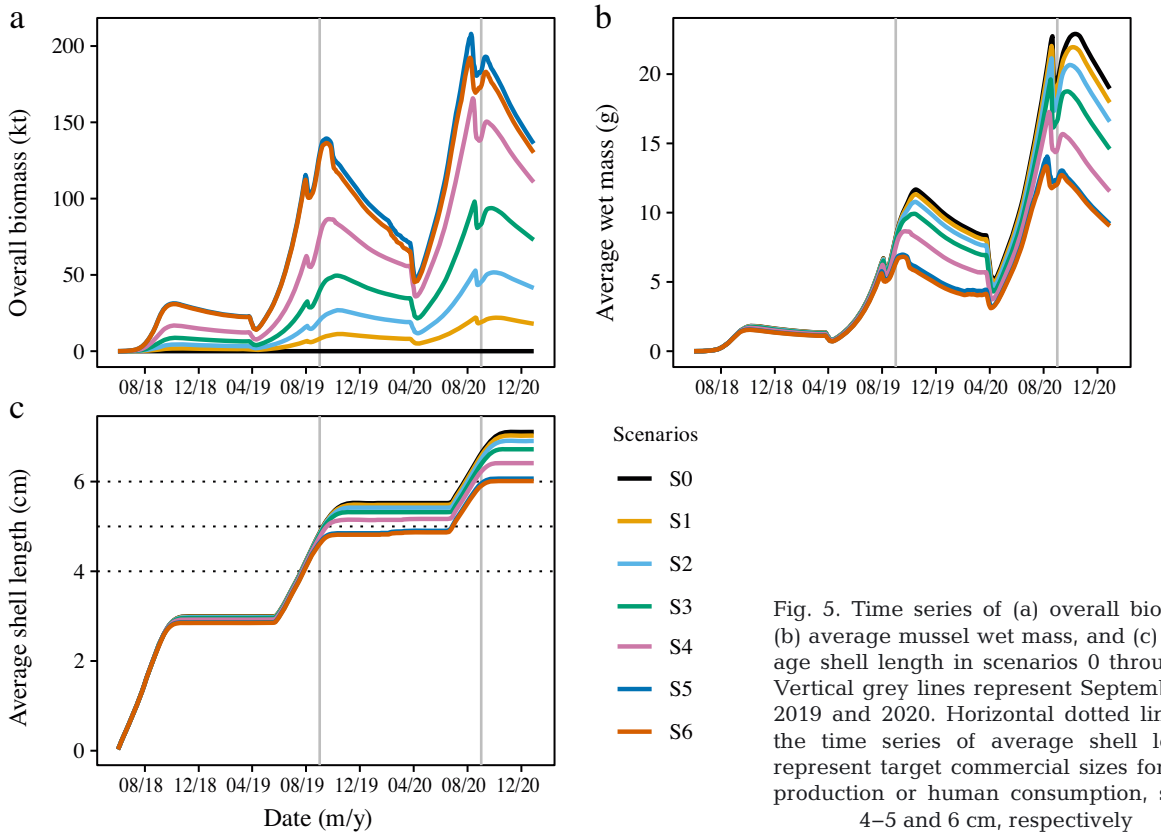

Fig. 5. Time series of (a) overall biomass, (b) average mussel wet mass, and (c) average shell length in scenarios 0 through 6. Vertical grey lines represent September 1, 2019 and 2020. Horizontal dotted lines in the time series of average shell length represent target commercial sizes for feed production or human consumption, set at 4–5 and 6 cm, respectively

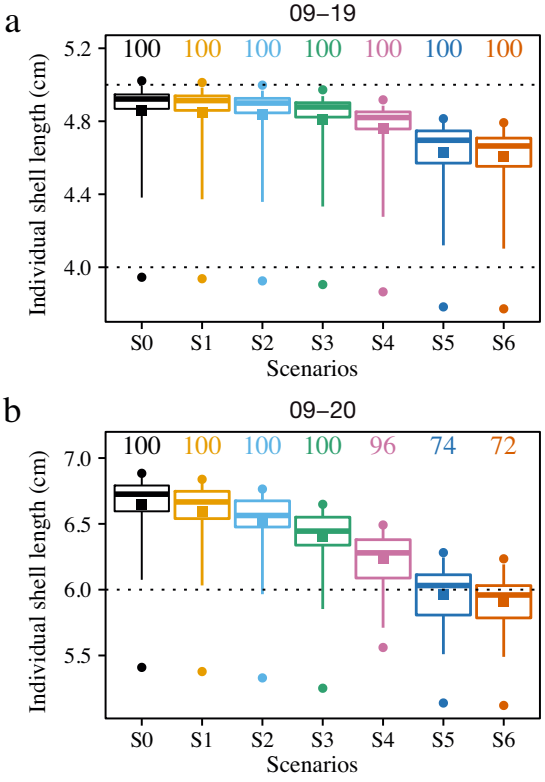

Fig. 6. Variability of individual shell length among farms on (a) September 1, 2019 and (b) September 1, 2020. Squares represent the mean, circles represent minimum and maximum values, thick horizontal lines within boxes represent median values, bottom and top of boxes represent 25 and 75% percentiles and whiskers represent 2.5 and 97.5% percentiles. The number of operable sites are shown at the top of the boxplots. Horizontal dotted lines represent target commercial sizes for feed production or human consumption, set at 4–5 and 6 cm, respectively

where mussels in numerous sites did not reach this target. In addition to lower growth, the most extreme scenarios, S5 and S6, displayed high starvation mortality (26 and 28% respectively) in the second year, thus reducing the number of operable farming sites for human consumption (Fig. 6).

The overall farm biomass ranged from 8.2 (S1) to 129.7 kt (S5) for feed production and from 19.2 (S1) to 184.4 kt (S5) for human consumption. Due to the combination of slower growth and a reduced number of productive sites caused by mortality, the increase in initial number of juveniles relative to S1 (10 million individuals) was no longer associated with proportional increase in production beyond S3 (50 million) and S2 (25 million) for feed production and human consumption, respectively. The comparison between S5 and S6 showed that the removal of salmon farms had little effect on average growth (–2 and –3% in wet mass for feed production and human consumption, respectively) and average farm biomass (–2 and –5%) at the scale of the whole fjord (Fig. 5). These decreases in biomass and growth were not uniform among mussel farms and were more marked in the vicinity of the salmon farms during fall and winter months (not shown).

3.3. Effect on the food web

The effect of the different farming scenarios on net primary production (NPP) remained low (<2% in S5 compared to S0, Fig. 8). Mean NPP for S0 in both 2019 and 2020 was 114 gC m^{-2} yr^{-1}, adding up to a

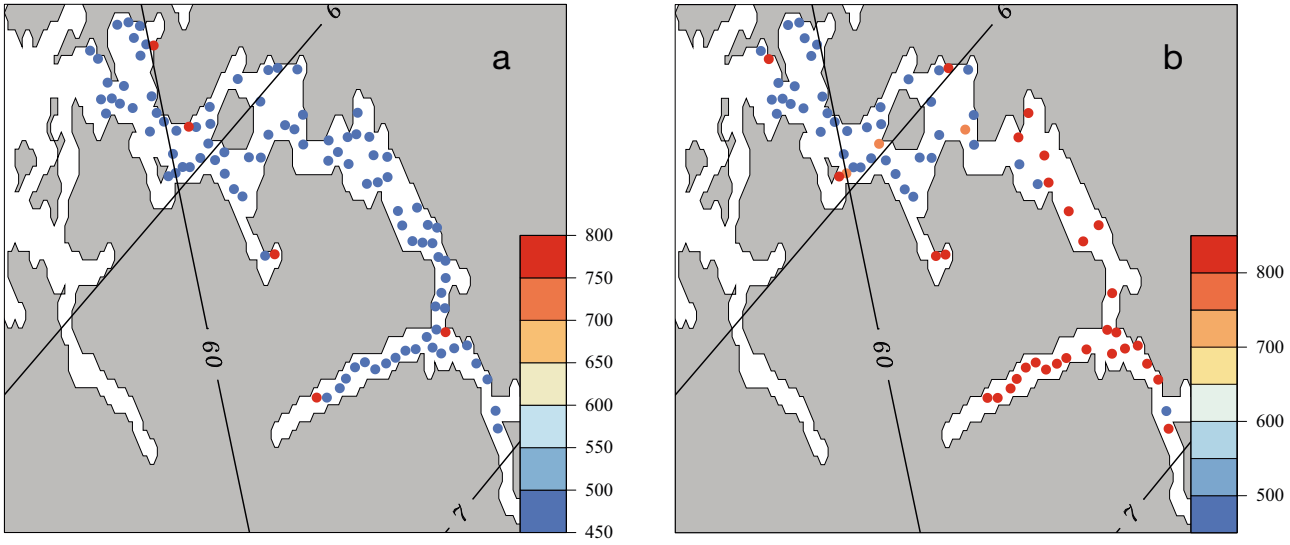

Fig. 7. Days required for each site to reach the minimum commercial size for feed production (5.0 cm) in (a) the reference simulation S0 and (b) S5. Note that the total number of farms is reduced in S5 as some have been removed due to starvation mortality

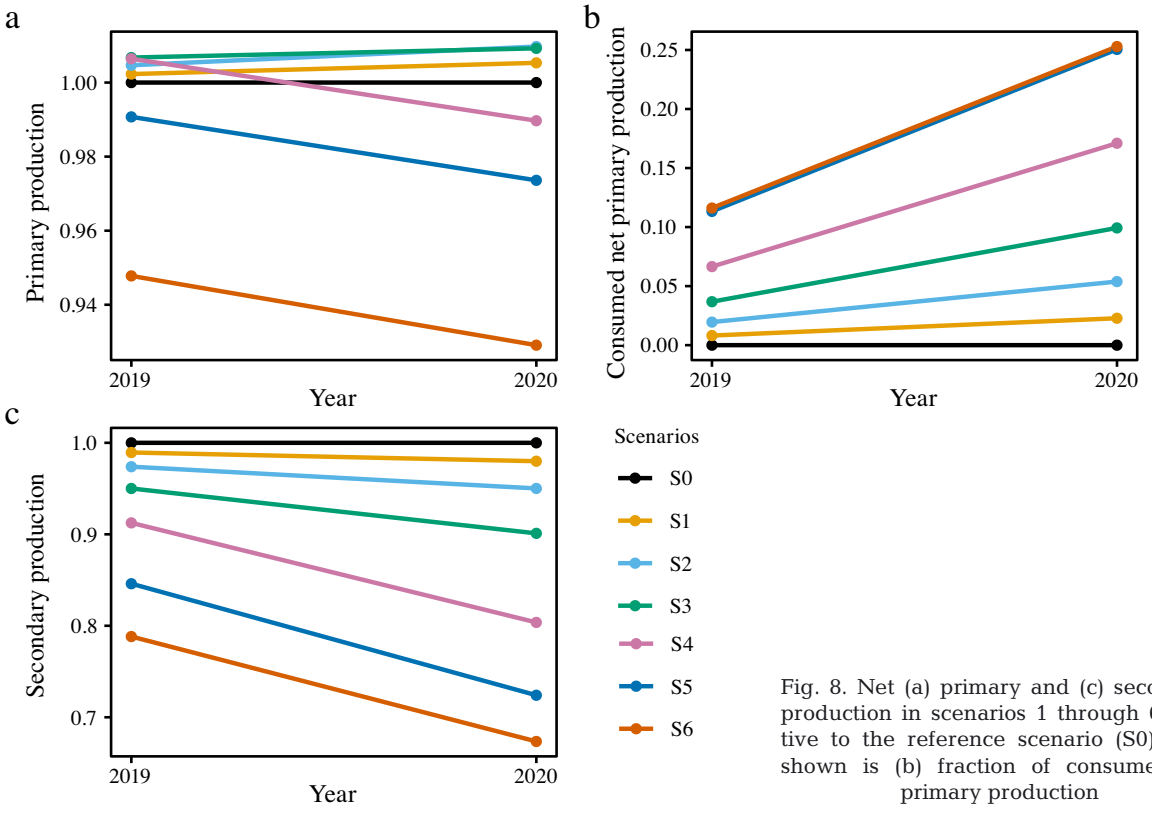

Fig. 8. Net (a) primary and (c) secondary production in scenarios 1 through 6 relative to the reference scenario (S0). Also shown is (b) fraction of consumed net primary production

total of 89 kt of carbon within the annotated box in Fig. 1. Even though NPP remained relatively unchanged, mussel feeding depleted up to 50–60 % of available phytoplankton biomass for both production for feed and human consumption in S4 and S5 (Fig. 9). Major phytoplankton depletion occurred during late summer and fall, and the highest annual consumption (S5) was equivalent to 12 and 25 % of NPP in 2019 and 2020 respectively (Fig. 8).

Consumption of phytoplankton biomass ranged from 0.5 (S1) to 8.5 kt (S5) of carbon for feed production and from 1.7 (S1) to 19.8 kt (S5) of carbon for human consumption (Fig. 10). Carbon retention in mussel flesh ranged from 36.9 (S6) to 38.7 % (S0) and from 23.8 (S6) to 27.4 % (S0) on September 1, 2019 and 2020, respectively. This metric displayed an overall decrease over time but remained almost unchanged among scenarios until August 2019; patterns differed more among scenarios during fall and winter months. In the cases of S5 and S6, mussels from numerous sites died of starvation in early 2020. We considered this dead biomass fixed in mussels; thus carbon retention from these 2 scenarios may be overestimated in 2020.

Annual zooplankton production (gC m^{-2} yr^{-1}) decreased by up to 21 and 33 % (S6) over 2019 and 2020 respectively (Fig. 8). The spatial change in annual zooplankton production is shown in Fig. 11. Changes can be seen across the entire Hardangerfjord, including outside the area where mussel farms are located. In 2019, production varied between a maximum decrease by 24 % to a slight increase in the inner part of the fjord fork (Sørfjorden). The mean difference within the annotated box in Fig. 1 is –9.0 %. For the second year (2020) the corresponding numbers are –35 % and –13.9 %.

4. DISCUSSION

In this study, a numerical modelling approach was used to explore the production capacity and associated food web interactions of mussel farming in a large mesotrophic fjord, using a set of simulations covering low to extensive production scales with 2 different applications: the production of feed for fish farming or the production of mussels for human consumption. While NORWECOM.E2E simulates high-resolution spatio-temporal oceanographic and biological processes (e.g. planktonic dynamics and nutrient recycling), the DEB-IBM predicts production estimates (growth, spawning, and starvation) of farmed mussels. The main strength of this combined modelling approach resides in a 2-way coupling, enabling assessment of both the direct grazing effect of mussels on the primary producers as well as the

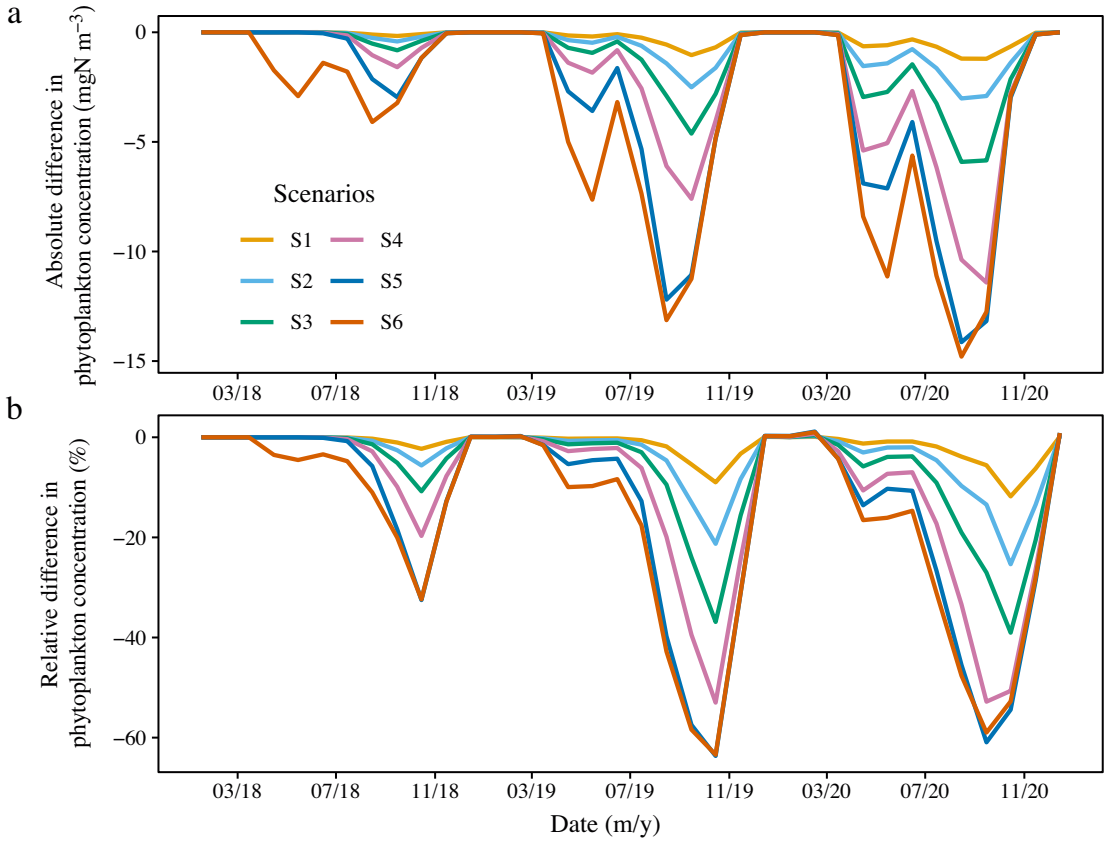

Fig. 9. Time series of (a) absolute and (b) relative phytoplankton concentration changes in scenarios 1 through 6, relative to the reference scenario (S0)

indirect effects through competition towards secondary producers and through nutrient recycling. This approach supports the exploration of favorable production sites and further optimization of their spatial distribution given a set of constraints such as physical properties (e.g. depth, current speed, distance from land) and/or the practical consideration of distancing among sites (both between mussel farms or between salmon and mussel farms).

Even though the present results depend on some model assumptions (e.g. spawning phenology or total shell length to shell free dry mass) and on the experimental set-up (starting date, time series of environmental forcing), this application provides a mechanistic understanding of the processes controlling the production capacity of the fjord and how extensive mussel farming might alter the basis of the food web.

4.1. Overall production potential

Within the range of tested farming intensity, overall farm biomass kept increasing as a function of the initial number of mussel juveniles up to 84 and 184 kt (scenario S6, total wet mass) for feed production and human consumption, respectively (Fig. 5). Although the increase was not proportional after S3 and S2, this suggests that the ultimate biomass production potential of the Hardangerfjord was not reached with our set of simulations. In addition, mussels reached commercial sizes in most scenarios, but this depends on the chosen target commercial sizes (4.0–5.0 cm for feed production and 6.0 cm for human consumption) used in this study. Increases in farming intensity were shown to decrease growth performance; thus if 5.0 cm is targeted for feed production instead of 4.0 cm, the production of suitable mussels for market may be delayed by anything between a few weeks up to the following productive season/year.

Increases in initial juvenile density not only reduced growth but also led to starvation in the most extreme scenarios (Fig. 6), highlighting the importance of food depletion and the possible detrimental effects on farms positioned downstream from other mussel farms. In the case of a production scheme designed for human consumption, in practice, there should be 2 ongoing production cycles lagged by 1 yr (2 cohorts) (Gangnery et al. 2004). A lower growth of

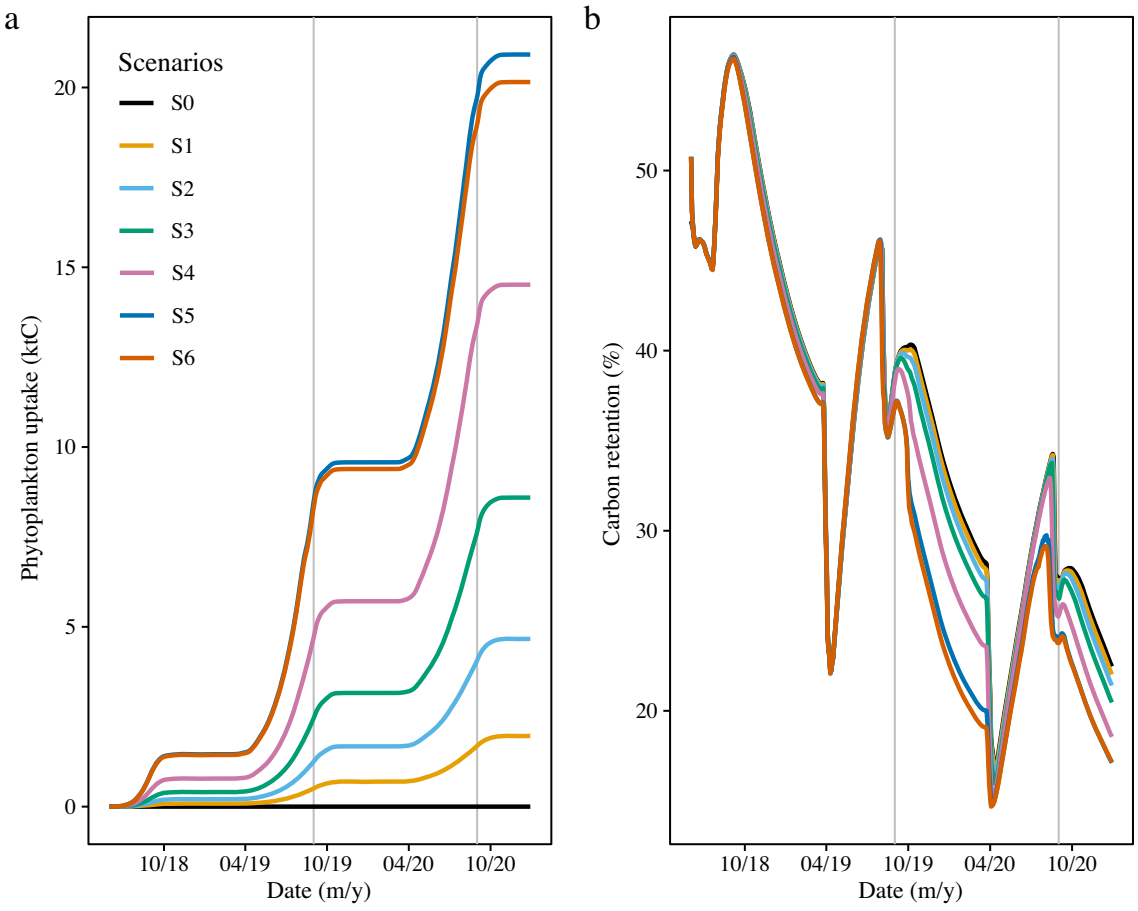

Fig. 10. Time series of (a) cumulative phytoplankton uptake and (b) carbon retention in scenarios 0 through 6. Vertical grey lines represent September 1, 2019 and September 1, 2020

mussels may be expected at high densities due to competition for food between the 2 cohorts. For feed production, where only 1 cohort is needed, the production potential was not reached in any scenario and seeding could therefore be increased several-fold to reach a biomass in the first year comparable to the biomass in the second year for human consumption. (Fig. 5).

The efficiency of carbon retention within mussel soft tissues decreased over time (Fig. 10), as larger mussels suffer from higher maintenance and reproduction costs. Thus, short production cycles may be

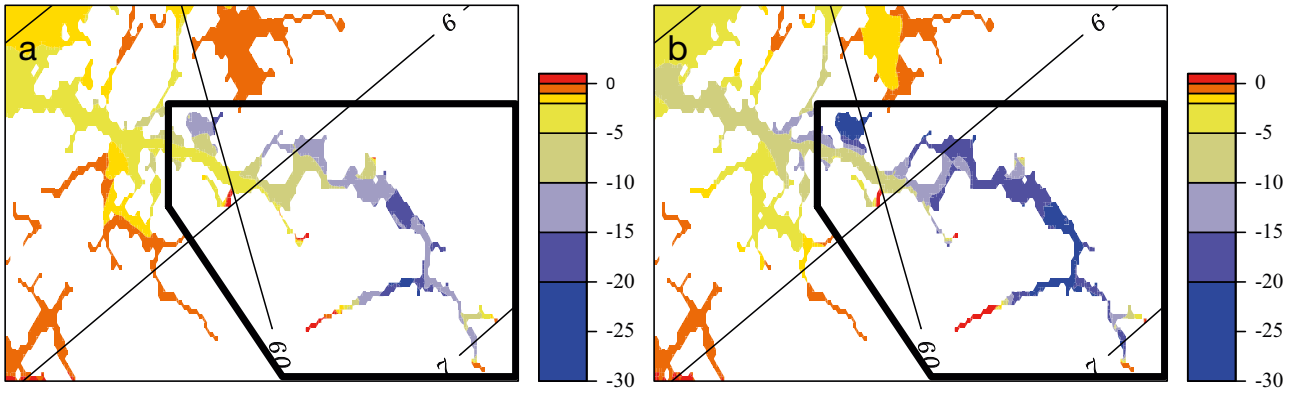

Fig. 11. Change (%) in annual secondary production for (a) 2019 and (b) 2020 between the reference simulation (S0) and the simulation with very high biomass (S5)

seen as more efficient from an energetic point of view. Production systems oriented toward feed production may thus be preferred over those aiming to produce mussels for human consumption. However, this neglects the feeding efficiency of fish in the upper trophic levels such as Atlantic salmon *Salmo salar*, which might feed on mussel meals. Thus, a more comprehensive life cycle analysis is needed to better assess the efficiency of both systems to deliver final products destined for human consumption. Apart from feeding efficiency in the upper trophic levels, consideration of economic viability and profitability is also required. As an example, we refer the reader to a recent study by Buer et al. (2020) for a detailed integration of operating costs and product market values for both farming purposes.

4.2. Site selection and interaction with salmon farming

The consistency of growth variability for all scenarios (Fig. 6) suggests that further optimization of mussel production within the fjord might require planning at much finer scales and possibly revising the farming design, such as establishing fewer but larger farms. In the present study, V was used as a proxy for growth and thereby site selection. However, for the final harvested products, both E and R are also important quality measures. Rosland et al. (2011) demonstrated spatial growth patterns of mussels farmed on longline structures using a spatially resolved model with boxes of 30 m length and width between 1 and 10 m for simulation of flow reduction, seston depletion and individual mussel growth (IBM-DEB) inside a longline mussel farm, based on farm configuration (spacing between longlines, farm length and stocking density) under a set of environmental conditions (data from the Hardangerfjord). Also, Taylor et al. (2021) showed interactions of both farm design and ambient environments at finer scales than in the present study in and around mussel farms (using model grid cells of 25 × 10 m^2) on particle depletion.

Including salmon farms when calculating the minimum distance between farming sites demonstrates how interactions between regulatory factors and our site selection criteria (current speed, depth, and distance to shore and other farms) affect both distribution of the 100 best sites and the production potential. A lower production potential of 8% when adding the distance constraint may indicate a degree of similarity of conditions for production throughout the fjord. However, distributing more farms in the inner part of the fjord may have associated effects not included in our study, like the effects of lower salinity on production (e.g. Maar et al. 2015, Buer et al. 2020) and increased risk of harmful algal blooms (Ramstad et al. 2001). Competition for space between mussel and salmon farms in the present study led to a slightly non-optimal selection of mussel farming sites. However, with respect to socioeconomic and spatial planning priorities, the economically more valuable salmon industry will probably have advantages, resulting in suboptimal sites being selected for mussel farming. Despite the amount of salmon farming within the fjord, its removal from the model has very little effect on the overall production of mussels, but this may hide more contrasts in the vicinity of the mussel farms at finer temporal scales. However, there is a consensus that extraction by bivalves (like mussels) of the horizontal flux of waste particles from open water cage finfish aquaculture is marginal. Increased growth will only occur very close to the cages and decrease quickly at distances much less than the spatial dimension of the cages (Strand et al. 2019). Alternative approaches have been suggested, like nutrient extraction of recirculated bay-scale trophic production, or extraction in the benthic environment below the cages where most of the organic waste ends up. Current configurations used in open water finfish culture suggest that adaptation of concepts allowing for better control of wastewater will enable longer contact times and thereby increased biogeochemical processing of the waste products (Filgueira et al. 2017, Strand et al. 2019). On the other hand, Maar et al. (2020, p. 339), in a study from the southwestern Kattegat, concluded that 'co-location of mussel farms with fish farm[s] was not advisable due to the negative benthic impact below the fish farms'. This consideration might put more constraints on the sites of mussel farms with respect to both depth and current speed.

4.3. Effect on the food web

The substantial impact of increased mussel farming biomass on zooplankton production in a fjord could potentially have very large impacts and cascade effects on the overall food web of mesotrophic fjord systems if extensive mussel farming is implemented (Gallardi 2014). Grazing activities from dense populations of mussels have a significant role in the energy and matter flow of estuarine and coastal ecosystems. Suspension feeders clear large water vol-

umes of particulate matter like phytoplankton and detritus and will also consume competitors for resources used by micro and mesozooplankton (Davenport et al. 2000, Prins & Escaravage 2005, Maar et al. 2007, Nielsen & Maar 2007). Therefore, grazing may induce depletion of both phytoplankton and zooplankton (Prins et al. 1997, Strohmeier et al. 2005, 2008, Maar et al. 2007, Cranford et al. 2016), and can also change the phytoplankton population and community structure through size-selective feeding. Traditionally there has been a purse seine fishery for sprat in several fjords in western Norway, and in 2019 the suggested quota in the Hardangerfjord was 500 t (https://www.fiskeridir.no). Sprat schools are mainly found in fjord branches and in the inner areas of the fjord, and copepods are among the most important prey of sprat in Hardangerfjord. A negative relationship between feeding activity in sprat and their zooplankton prey has been observed, indicating possible top-down control from non-larval sprat (Falkenhaug & Dalpadado 2014). In the nearby Masfjorden, the availability of zooplankton has been identified as a key factor in the carrying capacity of cod and its competitors (Fosså 1991, Salvanes et al. 1992). In the outer coastal areas, carrying capacity largely depends on the fluctuating advective processes, while in the inner areas (where the farms are localized) local zooplankton production contributes relatively more (Salvanes et al. 1995). Therefore, the large impact of intensive mussel farming on zooplankton communities in fjords may lead to extensive influence on the entire food web in fjords.

Under farming scenarios S4 and S5, during late summer and fall the mussels depleted more than half of the phytoplankton in the fjord (Fig. 9), which may increase the competition for food among grazers. The peak phytoplankton depletion coincides with a natural low abundance of phytoplankton, rapid mussel growth, high temperature, and increasing mussel biomass. The relative contribution of zooplankton to mussel diet is not well known, and zooplankton consumed by mussels (e.g. decreased competition) are not accounted for in the model. The up to 60% phytoplankton depletion in S5 on an ecosystem scale may induce a shift in phytoplankton composition towards picoplankton, as mussels show decreasing retention efficiency for particles smaller than 6–8 µm (Cranford et al. 2016). Observations of elevated picoplankton concentrations due to bivalve grazing have been reported from lagoons (Vaquer et al. 1996, Souchu et al. 2001), oyster ponds (Klaveness 1990), estuaries (Cranford et al. 2008, Smaal et al. 2013), and through a 20 km long strait (Norèn et al. 1999). A shift towards smaller algal cells would benefit grazers such as tunicates, which are able to retain smaller particles (Cranford et al. 2016). The model does not discriminate between sizes of phytoplankton; therefore the phytoplankton biomass available as food to farmed mussels may be overestimated, if picoplankton forms a large proportion of the total biomass. The ecosystem effects of depleted phytoplankton biomass or a shift in algal size are largely unknown.

Determination of the acceptable magnitude of impact on the food web remains beyond the scope of this study, although this will likely imply that the ecological carrying capacity of mussel farming may be below its production capacity. Along those lines, mussel production for feed may be considered less detrimental to the ecosystem since it would imply lower consumption of phytoplankton to produce the same amount of mussel biomass. For example, production under S4 in September 2019 is 75 kt with an accumulated phytoplankton uptake of 4.7 ktC, while under S3 in September 2020 the production is 84 kt with an uptake of 7.7 ktC.

In addition to food web effects through competition with zooplankton for prey, there is also a potential impact between farmed and wild populations of mussels. Fish and shellfish farming should not have any undesired effects on wild populations, such as genetic pollution, competition, and spread of diseases and parasites. The biomass of wild mussels in the Hardangerfjord has been estimated at ca. 13 kt (P. Gatti unpubl. data), which remains about an order of magnitude lower than the potential of the farmed standing stock within the fjord. Thus, farming may have effects on the spatio-temporal dynamics of wild stock.

5. CONCLUDING REMARKS

Bivalves have been suggested as candidates to meet the increasing need for new sustainable marine resources to support the demand for human food and ingredients in feed applications. The present study has shown how a numerical model can be used to assess the production capacity for such farming in a large mesotrophic fjord system, while at the same time assessing and quantifying food web interactions and environmental impacts. The Hardangerfjord already has extensive salmonid farming, and this study indicates that, while the 2 production regimes can co-exist with a possible positive but marginal feedback on mussel production from fish farming nutrient release, there is a possible conflict in terms

of the best sites for production. In showing that extensive mussel production will have a potential impact on zooplankton production and biomass, this study indicates the necessity of further studies to provide a stronger knowledge-based assessment of what is an acceptable ecological impact.

Nevertheless, while interpreting the results there are several issues to be kept in mind. This state-of-the-art modelling study is still limited by knowledge gaps and conflicting data. We have limited knowledge of spawning control of mussels, and while the seasonal window used in the model is in accordance with observations, actual spawning effort is greater in fall than in spring (not shown). In the model, all farms were initialized equally on the same date, while in a real world application, more realistic production schemes for optimized growth and economic value will be designed. This will have important impacts on some indicators, such as flesh content. Finally, in the present version of the DEB-IBM, growth is considered independent of salinity which could mask a gradient of growth from the inner to the outer fjord. This dependency should be added in future versions of the model.

The method used in this study is generalized and could be used elsewhere to help management by setting limits within which farming could be developed, and where the extent of impacts is considered acceptable. With such a modeling tool, it is also possible to integrate many more constraints or regulations associated with design of farming sites. To understand and project the consequences of multiple anthropogenic stressors, ecosystem models are probably the best tool. Models also allow a full investigation of system-wide cause–effect relationships. The use of observations and models in combination, therefore, allows for an improved assessment of both the state of the system, and the impact of cumulative stressors and their drivers (Skogen et al. 2021).

Acknowledgements. This work was financed by the Institute of Marine Research (internal project no. 15197 MORMOR) and the Norwegian Research Council (RCN project no 299554/F40, SIS-Sjømat).

LITERATURE CITED

Aksnes D, Ulvestad K, Baliño B, Berntsen J, Egge J, Svendsen E (1995) Ecological modelling in coastal waters: towards predictive physical-chemical-biological simulation models. Ophelia 41:5–36

ICES CM 2008/H:12 (2017) Food from the oceans: How can more food and biomass be obtained from the oceans in a way that does not deprive future generations of their benefits? Evidence Review Report No. 1. SAPEA, Berlin

Albrektsen S, Kortet R, Skov PV, Ytteborg E and others (2022) Future feed resources in sustainable salmonid production: a review. Rev Aquacult 14:1790–1812

Albretsen J, Sperrevik A, Staalstrøm A, Sandvik A, Vikebø F, Asplin L (2011) NorKyst-800 report no.1. User manual and technical description. Tech. Rep. Fisken og Havet 2-2011, Institute of Marine Research, Bergen

Asplin L, Johnsen I, Sandvik A, Albretsen J, Sundfjord V, Aure J, Boxaspen K (2014) Dispersion of salmon lice in the Hardangerfjord. Mar Biol Res 10:216–225

Asplin L, Albretsen J, Johnsen I, Sandvik A (2020) The hydrodynamic foundation for salmon-lice dispersion modeling along the Norwegian coast. Ocean Dyn 70: 1151–1167

Avdelas L, Avdic-Mravlje E, Borges Marques AC, Cano S and others (2021) The decline of mussel aquaculture in the European Union: causes, economic impacts, and opportunities. Rev Aquacult 13:91–118

Bernard I, de Kermoysan G, Pouvreau S (2011) Effect of phytoplankton and temperature on the reproduction of the pacific oyster *Crassostrea gigas*: investigation through DEB theory. J Sea Res 66:349–360

Bode A, Barquero S, Gonzales N, Alvarez-Ossorio M, Varela M (2004) Contribution of heterotrophic plankton to nitrogen regeneration in the upwelling ecosystem of La Coruna (NW Spain). J Plankton Res 26:11–28

Buer AL, Maar M, Nepf M, Ritzenhofen L and others (2020) Potential and feasibility of *Mytilus* spp. farming along a salinity gradient. Front Mar Sci 7:371

Cranford PJ, Li W, Strand Ø, Strohmeier T (2008) Phytoplankton depletion by mussel aquaculture: high resolution mapping, ecosystem modeling and potential indicators of ecological carrying capacity. ICES CM 2008/H:12

Cranford PJ, Strohmeier T, Filgueira R, Strand Ø (2016) Potential methodological influences on the determination of particle retention efficiency by suspension feeders: *Mytilus edulis* and *Ciona intestinalis*. Aquat Biol 25: 61–73

Davenport J, Smith RJ, Packer M (2000) Mussels *Mytilus edulis*: significant consumers and destroyers of mesozooplankton. Mar Ecol Prog Ser 198:131–137

Duinker A, Håland L, Hovgaard P, Mortensen S (2008) Gonad development and spawning in one- and two-year-old mussels (*Mytilus edulis*) from western Norway. J Mar Biol Assoc UK 88:1465–1473

Falkenhaug T, Dalpadado P (2014) Diet composition and food selectivity of sprat (*Sprattus sprattus*) in Hardangerfjord, Norway. Mar Biol Res 10:203–215

FAO (Food and Agriculture Organization of the United Nations) (2020) The state of world fisheries and aquaculture. FAO, Rome

Filgueira R, Guyondet T, Comeau LA, Grant J (2014) A fully spatial ecosystem-DEB model of oyster (*Crassostrea virginica*) carrying capacity in the Richibucto estuary, eastern Canada. J Mar Syst 136:42–54

Filgueira R, Guyondet T, Comeau LA, Sutherland TF (2016) Dynamic energy budget (DEB) models of bivalve molluscs inhabiting British Columbia coastal waters: review of existing data and further directions for data collection. Can Tech Rep Fish Aquat Sci 3173

Filgueira R, Guyondet T, Reid G, Grant J, Cranford P (2017) Vertical particle fluxes dominate integrated multi-trophic aquaculture (IMTA) sites: implications for shellfish-finfish synergy. Aquacult Environ Interact 9: 127–143

Filgueira R, Strople LC, Strohmeier T, Rastrick S, Strand Ø (2019) Mussels or tunicates: that is the question. Evaluating efficient and sustainable resource use by low-trophic species in aquaculture settings. J Clean Prod 231: 132–143

Fosså JH (1991) The ecology of the two-spot goby (*Gobiusculus flavescens fabricius*): the potential for cod enhancement. ICES Mar Sci Symp 192:147–155

Gallardi D (2014) Effects of bivalve aquaculture on the environment and their possible mitigation: a review. Fish Aquac J 5:105

Galparsoro I, Murillas A, Pinarbasi K, Sequeira AM and others (2020) Global stakeholder vision for ecosystem-based marine aquaculture expansion from coastal to offshore areas. Rev Aquacult 12:2061–2079

Gangnery A, Bacher C, Buestel D (2004) Application of a population dynamics model to the Mediterranean mussel, *Mytilus galloprovincialis*, reared in Thau Lagoon (France). Aquaculture 229:289–313

Gao S, Hjøllo S, Falkenhaug T, Strand E, Edwards M, Skogen MD (2021) Overwintering distribution, inflow patterns and sustainability of *Calanus finmarchicus* in the North Sea. Prog Oceanogr 194:102567

Garber J (1984) Laboratory study of nitrogen and phosphorus remineralization during decomposition of coastal plankton and seston. Estuar Coast Shelf Sci 18:685–702

Gatti P, Petitgas P, Huret M (2017) Comparing biological traits of anchovy and sardine in the Bay of Biscay: a modelling approach with the dynamic energy budget. Ecol Modell 348:93–109

Gehlen M, Malschaert H, Raaphorst W (1995) Spatial and temporal variability of benthic silica fluxes in the southeastern North Sea. Cont Shelf Res 15:1675–1696

Hjøllo S, Huse G, Skogen MD, Melle W (2012) Modelling secondary production in the Norwegian Sea with a fully coupled physical/primary production/individual-based *Calanus finmarchicus* model system. Mar Biol Res 8: 508–526

ICES (2022) Norwegian sea ecoregion — aquaculture overview. ICES, Copenhagen

Jansen HM, Strand Ø van Broekhoven W, Strohmeier T, Verdegem MC, Smaal AC (2019) Feedbacks from filter feeders: review on the role of mussels in cycling and storage of nutrients in oligo-meso-and eutrophic cultivation areas. In: Smaal AC, Ferreira JG, Grant J, Petersen JK, Strand Ø (eds) Goods and services of marine bivalves. Springer Nature, Cham, p 143–177

Johnsen IA, Fiksen Ø, Sandvik AD, Asplin L (2014) Vertical salmon lice behavior as a response to environmental conditions and its influence on regional dispersion in a fjord system. Aquacult Environ Interact 5:127–141

Klaveness D (1990) Size structure and potential food value of the plankton community to *Ostrea edulis L.* in a traditional Norwegian østerspoll. Aquaculture 86:231–247

Kooijman SALM (2010) Dynamic energy budget theory for metabolic organisation, 3rd edn. Cambridge University Press, New York, NY

Kotwicki L, Weslawski JM, Włodarska-Kowalczuk M, Mazurkiewicz M and others (2021) The re-appearance of the *Mytilus* spp. complex in Svalbard, Arctic, during the Holocene: the case for an arrival by anthropogenic flotsam. Global Planet Change 202:103502

Krause G, Buck BH, Breckwoldt A (2019) Socio-economic aspects of marine bivalve production. In: Smaal AC, Ferreira JG, Grant J, Petersen JK, Strand Ø (eds) Goods and services of marine bivalves. Springer Nature, Cham, p 317–334

Lavaud R, Guyondet T, Filgueira R, Tremblay R, Comeau LA (2020) Modelling bivalve culture — eutrophication interactions in shallow coastal ecosystems. Mar Pollut Bull 157:111282

Lika K, Kearney MR, Freitas V, van der Veer HW and others (2011a) The 'covariation method' for estimating the parameters of the standard dynamic energy budget model I: philosophy and approach. J Sea Res 66:270–277

Lika K, Kearney MR, Kooijman SA (2011b) The 'covariation method' for estimating the parameters of the standard dynamic energy budget model II: properties and preliminary patterns. J Sea Res 66:278–288

Lohse L, Malschaert F, Slomp C, Helder W, Raaphorst W (1995) Sediment-water fluxes of inorganic nitrogen compounds along the transport route of organic matter in the North Sea. Ophelia 41:173–197

Lohse L, Kloostechuis H, Raaphorst W, Helder W (1996) Denitrification rates as measured by the isotope pairing method and by the acetylene inhibition technique in continental shelf sediments of the North Sea. Mar Ecol Prog Ser 132:169–179

Maar M, Nielsen TG, Bolding K, Burchard H, Visser AW (2007) Grazing effects of blue mussel *Mytilus edulis* on the pelagic food web under different turbulence conditions. Mar Ecol Prog Ser 339:199–213

Maar M, Bolding K, Petersen JK, Hansen JLS, Timmermann K (2009) Local effects of blue mussels around turbine foundations in an ecosystem model of Nysted off-shore wind farm. J Sea Res 62:159–174

Maar M, Saurel C, Landes A, Dolmer P, Petersen JK (2015) Growth potential of blue mussels (*M. edulis*) exposed to different salinities evaluated by a dynamic energy budget model. J Mar Syst 148:48–55

Maar M, Larsen J, von Thenen M, Dahl K (2020) Site selection of mussel mitigation cultures in relation to efficient nutrient compensation of fish farming. Aquacult Environ Interact 12:339–358

Marques GM, Augustine S, Lika K, Pecquerie L, Domingos T, Kooijman SALM (2018) The AmP project: comparing species on the basis of dynamic energy budget parameters. PLOS Comput Biol 14:e1006100

Marques GM, Lika K, Augustine S, Pecquerie L, Kooijman SA (2019) Fitting multiple models to multiple data sets. J Sea Res 143:48–56

Martinsen E, Engedahl H (1987) Implementation and testing of a lateral boundary scheme as an open boundary condition in a barotropic ocean model. Coast Eng 11: 603–627

Mascorda Cabre L, Hosegood P, Attrill MJ, Bridger D, Sheehan EV (2021) Offshore longline mussel farms: a review of oceanographic and ecological interactions to inform future research needs, policy and management. Rev Aquaculture 13:1864–1887

Mayer B (1995) Ein dreidimensionales, numerisches Schwebstoff-Transportmodell mit Anwendung auf die Deutsche Bucht. Tech Rep GKSS 95/E/59, GKSS-Forschungszentrum Geesthacht GmbH

Moll A, Stegert C (2007) Modeling *Pseudocalanus elongatus* population dynamics embedded in a water column ecosystem model for the northern North Sea. J Mar Syst 64: 35–46

Nielsen TG, Maar M (2007) Effects of a blue mussel *Mytilus edulis* bed on vertical distribution and composition of the

pelagic food web. Mar Ecol Prog Ser 339:185–198
Norèn F, Haamer J, Lindahl O (1999) Changes in the plankton community passing a *Mytilus edulis* mussel bed. Mar Ecol Prog Ser 191:187–194
Norwegian Ministry of Trade, Industry and Fisheries (2015) Predictable and environmentally sustainable growth in Norwegian salmon and trout farming (Meld. St. 16 2014±2015). https://www.regjeringen.no/no/dokumenter/meld.-st.-16-2014-2015/id2401865/ (in Norwegian)
Palmer SCJ, Gernez PM, Thomas Y, Simis S, Miller PI, Glize P, Barillè L (2020) Remote sensing-driven pacific oyster (*Crassostrea gigas*) growth modeling to inform offshore aquaculture site selection. Front Mar Sci 6:802
Pätsch J, Kühn W, Moll A, Herman L (2009) ECOHAM4 user guide — ECOsystem model, HAMburg, version 4. Tech Rep 01-2009. Institut für Meereskunde, Hamburg
Pete R, Guyondet T, Bec B, Derolez V and others (2020) A box-model of carrying capacity of the Thau lagoon in the context of ecological status regulations and sustainable shellfish cultures. Ecol Modell 426:109049
Pipe R (1985) Seasonal cycles in and effects of starvation on egg development in *Mytilus edulis*. Mar Ecol Prog Ser 24:121–128
Pohlmann T, Puls W (1994) Currents and transport in water. In: Sündermann J (ed) Circulation and contaminant fluxes in the North Sea. Springer-Verlag, Berlin, p 345–402
Prins T, Escaravage V (2005) Can bivalve suspension-feeders affect pelagic food web structure? NATO Science Series IV: Earth and Environmental Series, Vol 47. Springer, Dordrecht
Prins TC, Smaal AC, Dame RF (1997) A review of the feedbacks between bivalve grazing and ecosystem processes. Aquat Ecol 31:349–359
R Core Team (2019) R: A language and environment for statistical computing. R Foundation for Statistical Computing, Vienna
Ramstad H, Hovgaard P, Yasumoto T, Larsen S, Aune T (2001) Monthly variations in diarrhetic toxins and yessotoxin in shellfish from coast to the inner part of the Sognefjord, Norway. Toxicon 39:1035–1043
Rey F, Noji T, Miller L (2000) Seasonal phytoplankton development and new production in the central Greenland Sea. Sarsia 85:329–344
Rosland R, Strand Ø, Alunno-Bruscia M, Bacher C, Strohmeier T (2009) Applying dynamic energy budget (DEB) theory to simulate growth and bio-energetics of blue mussels under low seston conditions. J Sea Res 62:49–61
Rosland R, Bacher C, Strand Ø, Aure J, Strohmeier T (2011) Modelling growth variability in longline mussel farms as a function of stocking density and farm design. J Sea Res 66:318–330
Salvanes AGV, Aksnes DL, Giske J (1992) Ecosystem model for evaluating potential cod production in a west Norwegian fjord. Mar Ecol Prog Ser 90:9–22
Salvanes AGV, Aksnes DL, Fosså J, Giske J (1995) Simulated carrying capacities of fish in Norwegian fjords. Fish Oceanogr 4:17–32
Sandvik A, Johnsen I, Myksvoll M, Sævik P, Skogen MD (2020) Prediction of the salmon lice infestation pressure in a Norwegian fjord. ICES J Mar Sci 77:746–756
Saraiva S, van der Meer J, Kooijman SALM, Ruardij P (2014) Bivalves: from individual to population modelling. J Sea Res 94:71–83
Saraiva S, Freitas V, Oźorio R, Rato A, Joaquim S, Matias D, Neves R (2020) Mechanistic approach for oyster growth prediction under contrasting culturing conditions. Aquaculture 522:735105
SAPEA (Science Advice for Policy by European Academies) (2017) Food from the oceans: How can more food and biomass be obtained from the oceans in a way that does not deprive future generations of their benefits? Evidence Review Report No. 1. SAPEA, Berlin
Scheffer M, Baveco J, de Angelis D, Rose K, van Nes E (1995) Super individuals a simple solution for modelling large populations on an individual basis. Ecol Modell 80: 161–170
Shchepetkin A, McWilliams J (2003) A method for computing horizontal pressure-gradient force in an oceanic model with a nonaligned vertical coordinate. J Geophys Res 108:3090
Shchepetkin A, McWilliams J (2005) The regional oceanic modeling system (ROMS): a split-explicit, free-surface, topography-following-coordinate oceanic model. Ocean Model 9:347–404
Skartveit A, Olseth JA (1986) Modelling slope irradiance at high latitudes. Sol Energy 36:333–344
Skartveit A, Olseth JA (1987) A model for the diffuse fraction of hourly global radiation. Sol Energy 38:271–274
Skogen MD, Svendsen E, Berntsen J, Aksnes D, Ulvestad K (1995) Modelling the primary production in the North Sea using a coupled three-dimensional physical chemical biological ocean model. Estuar Coast Shelf Sci 41:545–565
Skogen MD, Eknes M, Asplin L, Sandvik A (2009) Modelling the environmental effects of fish farming in a Norwegian fjord. Aquaculture 298:70–75
Skogen MD, Ji R, Akimova A, Daewel U and others (2021) Disclosing the truth: Are models better than observations? Mar Ecol Prog Ser 680:7–13
Smaal A, Schellekens T, van Stralen M, Kromkamp J (2013) Decrease of the carrying capacity of the Oosterschelde estuary (SW Delta, NL) for bivalve filter feeders due to overgrazing? Aquaculture 404-405:28–34
Souchu P, Vaquer A, Collos Y, Landrein S, Deslous-Paoli JM, Bibent B (2001) Influence of shellfish farming activities on the biogeochemical composition of the water column in Thau lagoon. Mar Ecol Prog Ser 218:141–152
Sprung M (1984a) Physiological energetics of mussel larvae (*Mytilus edulis*). I. Shell growth and biomass. Mar Ecol Prog Ser 17:283–293
Sprung M (1984b) Physiological energetics of mussel larvae (*Mytilus edulis*). II. Food uptake. Mar Ecol Prog Ser 17: 295–305
Sprung M (1984c) Physiological energetics of mussel larvae (*Mytilus edulis*). III. Respiration. Mar Ecol Prog Ser 18: 171–178
Sprung M (1984d) Physiological energetics of mussel larvae (*Mytilus edulis*). IV. Efficiencies. Mar Ecol Prog Ser 18: 179–186
Stegert C, Moll A, Kreus M (2009) Validation of the three-dimensional ECOHAM model in the German Bight for 2004 including population dynamics of *Pseudocalnus elongatus*. J Sea Res 62:1–15
Strand Ø, Vølstad JH (1997) The molluscan fisheries and culture of Norway. In: MacKenzie Jr CL, Burrell V, Rosenfield A, Hobart WL (eds) The history, present condition, and future of the molluscan fisheries of North and Central America and Europe. NOAA Tech Rep NMFS 129, p 7–24
Strand Ø, Jansen HM, Jiang Z, Robinson S (2019) Perspectives on bivalves providing regulating services in inte-

grated multi-trophic aquaculture. In: Smaal AC, Ferreira JG, Grant J, Petersen JK, Strand Ø (eds) Goods and services of marine bivalves. Springer Nature, Cham, p 209–230

Strohmeier T, Aure J, Duinker A, Castberg T, Svardal A, Strand Ø (2005) Flow reduction, seston depletion, meat content and distribution of diarrhetic shellfish toxins in a long-line blue mussel (*Mytilus edulis*) farm. J Shellfish Res 24:15–23

Strohmeier T, Duinker A, Strand Ø, Aure J (2008) Temporal and spatial variation in food availability and meat ratio in a longline mussel farm (*Mytilus edulis*). Aquaculture 276: 83–90

Strohmeier T, Strand Ø, Cranford P (2009) Clearance rates of the great scallop (*Pecten maximus*) and blue mussel (*Mytilus edulis*) at low natural seston concentrations. Mar Biol 156:1781–1795

Taylor D, Larsen J, Buer AL, Friedland R and others (2021) Mechanisms influencing particle depletion in and around mussel farms in different environments. Ecol Indic 122:107304

Thomas JBE, Sinha R, Strand Ø, Söderqvist T and others (2022) Marine biomass for a circular blue-green bioeconomy? A life cycle perspective on closing nitrogen and phosphorus land-marine loops. J Ind Ecol: 26:2136–2153

Thomas Y, Razafimahefa NR, Mènesguen A, Bacher C (2020) Multi-scale interaction processes modulate the population response of a benthic species to global warming. Ecol Modell 436:109295

Torrissen O, Norberg B, Viswanath K, Strohmeier T, Strand Ø, Naustvoll L, Svåsand T (2018) Framtidsrettet matproduksjon i kyst og fjord — en vurdering av muligheter for økt sjømatproduksjon i Norge. Tech Rep Rapport fra Havforskningen, 23-2018. Institute of Marine Research, Bergen

Utne K, Hjøllo S, Huse G, Skogen MD (2012) Estimating consumption of *Calanus finmarchicus* by planktivorous fish in the Norwegian Sea using a fully coupled 3D model system. Mar Biol Res 8:527–547

Vaquer A, Troussellier M, Courties C, Bibent B (1996) Standing stock and dynamics of picophytoplankton in the Thau lagoon (northwest Mediterranean coast). Limnol Oceanogr 41:1821–1828

Wijsman JWM, Troost K, Fang J, Roncarati A (2019) Global production of marine bivalves. Trends and challenges. In: Smaal AC, Ferreira JG, Grant J, Petersen JK, Strand Ø (eds) Goods and services of marine bivalves. Springer Nature, Cham, p 7–26

Willer DF, Aldridge DC (2020) Sustainable bivalve farming can deliver food security in the tropics. Nat Food 1: 384–388

Willer DF, Nicholls RJ, Aldridge DC (2021) Opportunities and challenges for upscaled global bivalve seafood production. Nat Food 2:935–943

Editorial responsibility: Jonathan Grant, Halifax, Nova Scotia, Canada
Reviewed by: T. Prins and 2 anonymous referees

Submitted: June 20, 2022
Accepted: November 14, 2022
Proofs received from author(s): January 9, 2023